Medical Oncology (2019) 36:5
https://doi.org/10.1007/s12032-018-1225-1

ORIGINAL PAPER

The c-MYC/NAMPT/SIRT1 feedback loop is activated in early classical and serrated route colorectal cancer and represents a therapeutic target

Lydia Brandl[1] · Nina Kirstein[2] · Jens Neumann[1] · Andrea Sendelhofert[1] · Michael Vieth[3] · Thomas Kirchner[1,4] · Antje Menssen[2]

Received: 24 September 2018 / Accepted: 6 November 2018 / Published online: 20 November 2018

Abstract

We have recently identified a positive feedback loop in which c-MYC increases silent information regulator 1 (SIRT1) protein level and activity through transcriptional activation of nicotinamide phosphoribosyltransferase (*NAMPT*) and NAD^+ increase. Here, we determined the relevance of the c-MYC–NAMPT–SIRT1 feedback loop, including the SIRT1 inhibitor deleted in breast cancer 1 (DBC1), for the development of conventional and serrated colorectal adenomas. Immunohistochemical analyses of 104 conventional adenomas with low- and high-grade dysplasia and of 157 serrated lesions revealed that elevated expression of c-MYC, NAMPT, and SIRT1 characterized all conventional and serrated adenomas, whereas DBC1 was not differentially regulated. Analyzing publicly available pharmacogenomic databases from 43 colorectal cancer cell lines demonstrated that responsiveness towards a NAMPT inhibitor was significantly associated with alterations in *PTEN* and *TGFBR2*, while features such as *BRAF* or *RNF43* alterations, or microsatellite instability typical for serrated route colorectal cancer, showed increased sensitivities for inhibition of NAMPT and SIRT1. Our findings suggest an activation of the c-MYC–NAMPT–SIRT1 feedback loop that may crucially contribute to initiation and development of both routes to colorectal cancer. Targeting of NAMPT or SIRT1 may represent novel therapeutic strategies with putative higher sensitivity of the serrated route colorectal cancer subtype.

Keywords c-MYC · NAMPT · SIRT1 · Colorectal carcinogenesis · Analysis of pharmacogenomics databases

Introduction

Deregulation of the Wnt/ß-catenin signaling pathway leads to the development of sporadic colorectal carcinomas, that evolve via the classical adenoma–carcinoma sequence [1]. A crucial downstream transcriptional target of Wnt/ß-catenin signaling is the *c-MYC* proto-oncogene. By transcriptional induction or repression of target genes, c-MYC regulates cell cycle progression, cell growth, DNA replication, cellular metabolism, differentiation, and apoptosis and mediates many hallmark characteristics of cancer cells, reviewed in [2]. We and others have previously identified a positive feedback loop connecting c-MYC and n-MYC to the NAD^+-dependent protein deacetylase SIRT1 (silent information regulator 1), reviewed in [3]. c-MYC requires the function of nicotinamide phosphoribosyltransferase (NAMPT), that leads to increased NAD^+ to mediate SIRT1 activation [4]. SIRT1 regulates processes such as stress resistance, chromatin modification, proliferation, and cellular

Electronic supplementary material The online version of this article (https://doi.org/10.1007/s12032-018-1225-1) contains supplementary material, which is available to authorized users.

✉ Antje Menssen
menssenantje@gmail.com

1 Department of Pathology, Ludwig-Maximilians University (LMU), Thalkirchnerstraße 36, 80337 Munich, Germany

2 Research group "Signaling pathways in colorectal cancer", Department of Pathology, Ludwig-Maximilians University (LMU), Thalkirchnerstraße 36, 80337 Munich, Germany

3 Department of Pathology, Klinikum Bayreuth, Preuschwitzer Str. 101, 95445 Bayreuth, Germany

4 German Consortium for Translational Cancer Research (DKTK), DKTK site Munich, DKFZ, Im Neuenheimer Feld 280, 69120 Heidelberg, Germany

metabolism. Furthermore, SIRT1 negatively regulates p53 and other pro-apoptotic factors, and thereby antagonizes cellular senescence and inhibits apoptosis. We and others have shown that SIRT1 increases c-MYC activity, and is required for survival of cancer cells and cancer stem cells.

SIRT1 is highly expressed in colorectal tumors [5], and SIRT1 was shown to contribute to intestinal tumorigensis in mice [6]. We have demonstrated that elevated SIRT1 levels are associated with high c-MYC expression [4]. Additionally, we have shown that high SIRT1 and c-MYC levels are associated with oncogenic *BRAF* and *KRAS*, and also with activated Wnt signaling in serrated tumors of the colon [7]. With higher grades of malignancy and invasiveness, the expression of c-MYC and SIRT1 consistently increases, implicating a so far unrecognized role of c-MYC–SIRT1 feedback loop in the tumorigenesis of the serrated route to colorectal cancer (CRC) [7].

In recent years, the serrated route has emerged as an alternative route in the development of CRC comprising lesions with "saw-tooth" crypt morphology like hyperplastic polyps, sessile-serrated adenoma, traditional-serrated adenoma, and invasive-serrated adenocarcinomas. Initiating events in the formation of serrated lesions are mutations of *BRAF*, and less often *KRAS*, whereas activation of the Wnt/ß-catenin pathway is rare. Tumors exhibiting *BRAF* mutations are preferentially detected in the right colon and frequently exhibit DNA hypermethylation and microsatellite instability (MSI). In contrast, lesions with *KRAS* mutation are more often located in the left colon and are associated with microsatellite stability (MSS) or low MSI. Furthermore, there is a third group of serrated lesions which do not show any known aberrant oncogene activation (reviewed in [8]).

We studied the relevance of the c-MYC–NAMPT–SIRT1–DBC1 feedback loop for the development of early conventional adenomas and serrated lesions. Our results demonstrate a putative activation of the c-MYC, NAMPT, and SIRT1 feedback loop in early colorectal carcinogenesis. As therapeutic targeting of NAMPT and SIRT1 demonstrated efficacy in different tumor types in pre-clinical studies (reviewed in [9, 10]), we took advantage of resources for comprehensively associating drug sensitivities with molecular alterations of cancer cell lines (large databases are now available from the Broad-Novartis Cancer Cell Line Encyclopedia (CCLE) [11] and from the Genomics of Drug Sensitivity in Cancer (GDSC) project [12, 13]). Analyzing these pharmacogenomic databases, we show that interference with the c-MYC–NAMPT–SIRT1 positive feedback loop represents a novel therapeutic strategy, especially for serrated route CRC. While inactivating genetic alterations in *PTEN* and *TGFBR2* were significantly associated with sensitivity towards NAMPT inhibition, increased resistance to SIRT1 inhibition was linked with mutant and/or deleted *APC, FBXW7*, and *SMAD4*. Cell lines harboring genetic alterations typical for serrated route CRC such as altered *RNF43*, mutant *BRAF*, and MSI had a higher responsiveness to both drugs. The identified associations represent new stratification criteria for putatively responsive tumors for future clinical trials.

Materials and methods

Specimens

Formalin-fixed paraffin-embedded (FFPE) patient tissue was obtained from the archives of the Department of Pathology, Ludwig-Maximilians University, Munich. Altogether, 104 classical colorectal adenomas, and 157 serrated lesions were analyzed. Classical adenomas were assessed applying the criteria of the World Health Organization (WHO) [14]. All serrated samples probes were categorized by two independent pathologists (T.K. and L.B.) using the parameters established by Torlakovic et al. [15]. Our study comprised tubular adenomas with low- and high-grade dysplasia, tubulovillous adenomas with low and high-grade dysplasia, villous adenomas with low and high-grade dysplasia, hyperplastic polyps, sessile-serrated adenomas without intraepithelial neoplasia, sessile-serrated adenomas with low and high-grade intraepithelial neoplasia, and traditional-serrated adenomas with low and high-grade intraepithelial neoplasia (Tables 1, 2, and 3).

Immunohistochemistry

Immunohistochemical (IHC) staining was done on 3 µm consecutive tissue sections of FFPE tumor samples applying standard IHC protocols (for details see Online Resource 1). All primary antibody incubations were conducted at room temperature for one hour. Hematoxylin (Vector Laboratories, Cat. No. H-3401) was applied as counterstaining for all slides. System controls without primary antibodies as well as immunoglobulin isotype control antibodies were used to approve staining specificity. In addition, to confirm SIRT1 and NAMPT antibody specificity, HCT116 colorectal cancer cells were subjected to siRNA-mediated knockdown of *SIRT1* or *NAMPT* transcripts. Seventy-two hours post-transfection cells were scrapped, embedded in agarose, formalin fixed, dehydrated, and paraffin embedded. SIRT1 and NAMPT IHC staining of knockdown cells was negative compared to cells transfected with scrambled siRNA thus demonstrating specific staining of the antibodies.

c-MYC expression was evaluated regarding the number of nuclear positive cells and scored as 0 for 0% positive cells, 1–30% positive cells as score 1, 31–60% positive cells as score 2, and 61–100% positive cells as score 3. SIRT1 and DBC expression were evaluated regarding their nuclear

Table 1 Distribution of location of conventional adenomas, *KRAS* mutations, and age of patients

Histology	Number of cases (*n*)	Right sided	Left sided	Location n.a.	*KRAS* mutation (*n*)	Average age (year)	Age range (year)
Tubular adenoma LGIEN	28	15/28 (54%)	11/28 (39%)	2/28 (7%)	2/28 (7%)	66	33–82
Tubular adenoma HGIEN	10	4/10 (40%)	6/10 (60%)	–	2/10 (20%)	71	43–92
Tubulovillous adenoma LGIEN	23	10/23 (43%)	11/23 (48%)	2/23 (9%)	9/23 (39%)	65	46–83
Tubulovillous adenoma HGIEN	20	6/20 (30%)	13/20 (65%)	1/20 (5%)	9/20 (45%)	69	50–92
Villous adenoma LGIEN	14	3/14 (21%)	11/14 (79%)	–	7/14 (50%)	65	53–83
Villous adenoma HGIEN	9	0/9 (0%)	9/9 (100%)	–	6/9 (67%)	71	59–90
All adenomas	104	38/104 (37%)	61/104 (59%)	5/104 (4%)	35/104 (34%)	71	33–92

LGIEN low-grade intraepithelial neoplasia, *HGIEN* high-grade intraepithelial neoplasia, *n.a.* not applicable

positivity and NAMPT expression regarding its cytoplasmic and/or nuclear positivity.

Analyses of *KRAS*-/*BRAF* mutations

KRAS exon 2 codon 12/13 mutational status was determined for all microdissected serrated lesions and classical adenomas, and *BRAF*(V600E) exon 15 mutations were additionally assessed for all serrated lesions as described recently [7].

Statistical analysis

Cross tabulations were calculated using Fisher's exact test. Statistics were calculated using SPSS version 25.0 (SPSS Inc.). p-values < 0.05 were considered as statistically significant.

Data acquisition and availability

Datasets of CRC cell line mutation, copy number alteration, and mRNA expression were obtained from the cancer cell line encyclopedia (CCLE) database. The datasets analyzed during the current study are available at https://data.broadinstitute.org/ccle/CCLE_RNAseq_081117.rpkm.gct and for copy number alteration (cna) file:https://data.broadinstitute.org/ccle_legacy_data/dna_copy_number/CCLE_copynumber_byGene_2013-12-03.txt.

For cna, we inversed the normalized log2 ratios ($2^{CN} \times 2$) to obtain values directly corresponding to the copy number N (2 = 2N, 4 = 4N, 1 = 1N). We set the threshold for copy number gain (amplification) to 2.5, for copy number loss (deletion) to 1.5. Information on the mutation status is available for fifty CRC cell lines (Online Resource 2 for detailed information on positions of amino acid changes), and cna and gene expression data were obtained from 43 CRC cell lines (Online Resource 3). We selected the most frequently mutated genes in colorectal cancer [16], complemented for frequently mutated pathway-related genes and the gene *RNF43*, which is commonly mutated in serrated route CRC [17]. For our analyses, we selected only those genes mutated in over 5% of CRC patients according to the Cancer Genome Atlas Network study [16], resulting in a list of 26 recurrently somatically mutated genes. To determine the gene status, we combined mutation and copy number alteration data. The selected genes were grouped in either oncogene (*BRAF, CTNNB1, ERBB2, ERBB3, KRAS, NRAS, PIK3CA, SLC9A9*) or tumor suppressor gene (*ACVR2A, AMER1, APC, ARID1A, ATM, AXIN2, CDKN2A, FBXW7, MSH3, MSH6, PTEN, RNF43, SMAD2, SMAD4, SOX9, TCF7L2, TGFBR2, TP53*) according to the Cancer Genome Atlas Network [16], Slattery *et al.* [18] and Ueda *et al.* for classification of *SLC9A9* [19]. Information on MSI status and CpG island methylator phenotype (CIMP) phenotype of the cell lines was obtained from the following sources: [20, 21] and Cosmic (http://cancer.sanger.ac.uk/cell_lines). For a complete overview of the mutational and copy number alteration status of the 26 genes, MSI and CIMP, see also Online Resource 3. IC-50 values for FK866 and EX527 of CRC cell lines were downloaded from Genomics of Drug Sensitivity in Cancer (GDSC) (release 6.1 March 2017), selecting "COREAD" cancer type: FK866: http://www.cancerrxgene.org/translation/Drug/1248, EX527: http://www.cancerrxgene.org/translation/Drug/341. For further details concerning the drug screening procedure, visit http://www.cancerrxgene.org/help#t_curve. Processing datasets and statistical analyses were performed in R version 3.4.1, visualizations were done with GraphPad Prism 5 software.

Results

Classification, clinical data, and *KRAS* mutational status of classical colorectal adenomas

The final case compilation of classical colorectal adenomas comprised 104 lesions. Mutant *KRAS* was present in 35/104 (34%) cases. *KRAS* mutations were rare in tubular

Table 2 Distribution of location and *BRAF*/*KRAS* mutational status of serrated lesions and age of patients

Histology	Number of cases (*n*)	Right sided	Left sided	Location n.a.	*BRAF* mutation (*n*)		*KRAS* mutation (*n*)	*BRAF*/*KRAS* wt (*n*)	Average age (year)		Age range (year)
HP	27	12/27 (44%)	15/27 (56%)	–	21/27 (78%)		3/27 (11%)	3/27 (11%)	64		47–85
SSA	52	15/52 (29%)	36/52 (69%)	1/52 (2%)	38/52 (73%)		1/52 (2%)	13/52 (25%)	62		30–89
SSA with LGIEN	16	11/16 (69%)	3/16 (19%)	2/16 (12%)	10/16 (63%)	1/16 (6%)		5/16 (31%)	67	51–83	
SSA with HGIEN	22	14/22 (64%)	2/22 (9%)	6/22 (27%)	16/22 (73%)		1/22 (4%)	5/22 (23%)	70		51–92
TSA	28	8/28 (28%)	17/28 (61%)	3/28 (11%)	13/28 (46%)		12/28 (43%)	3/28 (11%)	68		46–89
TSA with HGIEN	12	4/12 (33%)	5/12 (42%)	3/12 (25%)	2/12 (17%)		6/12 (50%)	4/12 (33%)	73		57–86
All serrated lesions	157	64/157 (41%)	78/157 (50%)	15/157 (9%)	100/157 (64%)		24/157 (15%)	33/157 (21%)	66		30–92

HP hyperplastic polyp, *SSA* sessile-serrated adenoma, *TSA* traditional-serrated adenoma, *LGIEN* low-grade intraepithelial neoplasia, *HGIEN* high-grade intraepithelial neoplasia, *wt* wild-type, *n.a.* not applicable

adenomas with low and high-grade dysplasia (2/28 (7%) and 2/10 (20%)), more frequent in tubulovillous adenomas with low and high-grade dysplasia (9/23 (39%), and 9/20 (45%)), respectively, and most prevalent in villous adenomas with low and high-grade dysplasia (7/14 (50%) and 6/9 (67%)). The correlation of the type of adenoma with the *KRAS* mutational status was statistically significant ($p = 0.004$) and in accordance with the literature [22]. Table 1 summarizes location, age, and *KRAS* mutational status of patients' tumors.

Classification, clinical data, and *KRAS* and *BRAF* mutational status of serrated lesions

The final collection included 157 serrated lesions. Of these, 100/157 (64%) cases revealed a mutation in *BRAF*, and 24/157 (15%) cases a *KRAS* mutation. *BRAF* and *KRAS* mutations were mutually exclusive. 33/157 (21%) cases had neither a *BRAF* nor a *KRAS* mutation. Table 2 gives a summary of the type of lesion, *KRAS* and *BRAF* mutational status, location, and age of patients.

Sessile-serrated lesions with and without intraepithelial neoplasia were detected in the colon (44% (40/90) right sided vs. 46% (41/90) left sided) with frequent *BRAF* mutation (71% (64/90) *BRAF* vs. 1.1% (1/90) *KRAS* mutation). Traditional-serrated adenomas with low- and high-grade intraepithelial neoplasia occurred preferentially in the distal colon (30% (12/40) right sided vs. 55% (22/40) left sided) and showed more often *KRAS* mutations than sessile-serrated adenomas (45% (18/40) vs. 1.1% (1/90) *KRAS* mutation). Thus, our collection was representative of the previously observed distributions and frequencies [8].

NAMPT and DBC1 are expressed in epithelial cells of normal colon mucosa

In normal colorectal mucosa, we previously found c-MYC and SIRT1 expression restricted to the proliferative zone of the crypts [7]. To complement this observation for NAMPT and DBC1, we now also assessed the expression of these proteins in normal colorectal mucosa by immunohistochemistry. Unexpectedly, cytoplasmic and nuclear NAMPT were expressed in epithelial cells throughout the crypts from the proliferative zone to the upper parts, pointing to a physiological function of NAMPT in intestinal epithelial cells (Fig. 1a, b). Likewise, DBC1 was expressed in nuclei of all epithelial cells.

Table 3 Correlation of c-MYC protein expression to *KRAS* mutational status in conventional colorectal adenomas

Histology	c-MYC score 1		c-MYC score 2		c-MYC score 3		Total *KRAS* mut. cases
	Total	*KRAS* mut.	Total	*KRAS* mut.	Total	*KRAS* mut.	
Tubular adenoma							
LGIEN $n=28$	8/28 (29%)	1/28 (3.5%)	16/28 (57%)	1/28 (3.5%)	4/28 (14%)	0/28 (0%)	2/28 (7%)
HGIEN $n=10$	0/10 (0%)	0/10 (0%)	2/10 (20%)	1/10 (10%)	8/10 (80%)	1/10 (10%)	2/10 (20%)
Tubulovillous adenoma							
LGIEN $n=23$	9/23 (39%)	5/23 (22%)	8/23 (35%)	2/23 (9%)	6/23 (26%)	2/23 (9%)	9/23 (40%)
HGIEN $n=20$	3/20 (15%)	1/20 (5%)	0/20 (0%)	0/20 (0%)	17/20 (85%)	8/20 (40%)	9/20 (45%)
Villous adenoma							
LGIEN $n=14$	1/14 (7%)	1/14 (7%)	6/14 (43%)	4/14 (29%)	7/14 (50%)	2/14 (14%)	7/14 (50%)
HGIEN $n=9$	1/9 (11%)	0/9 (0%)	2/9 (22%)	2/9 (22%)	6/9 (67%)	4/9 (44%)	6/9 (66%)
All adenomas							
$n=104$	22/104 (21%)	8/104 (8%)	34/104 (33%)	10/104 (10%)	48/104 (46%)	17/104 (16%)	35/104 (34%)

The table gives the total number and percentage of classical adenoma cases with the respective c-MYC IHC score and KRAS mutational status
LGIEN low-grade intraepithelial neoplasia, *HGIEN* high-grade intraepithelial neoplasia

c-MYC, NAMPT, SIRT1, and DBC1 are highly expressed in all types of classical colorectal adenomas

To determine c-MYC, NAMPT, SIRT1, and DBC1 expression levels in classical colorectal adenomas, we performed IHC staining of these proteins in tubular adenomas with low-grade intraepithelial neoplasia (representative example shown in Fig. 2a–d), and tubular adenomas with high-grade intraepithelial neoplasia (Fig. 3a–d). In general, the proteins were highly expressed in all adenoma subtypes.

In classical colorectal adenomas, nuclear positivity of c-MYC ranged from 5% (score 1) to 90% (score 3) in individual cases. In tubular adenomas with low-grade intraepithelial neoplasia, low to intermediate (score 1 and score 2) c-MYC expression was detected in 86% (24/28) of cases, while 14% (4/28) expressed high c-MYC levels (score 3) (Table 3). Apical areas of low-grade adenomas exhibited higher expression of c-MYC than basal regions (Fig. 2a). NAMPT was expressed mainly in the cytoplasm of basal areas (Fig. 2b, high-magnification inset 1) and in the nucleus in apical regions (Fig. 2b, high-magnification inset 2) of tubular adenomas with low-grade intraepithelial neoplasia. Almost all dysplastic cells expressed SIRT1 (Fig. 2c) and DBC1 (Fig. 2d).

In tubular adenomas with high-grade intraepithelial neoplasia, all of 10 cases displayed high c-MYC expression (Fig. 3a) (score 2 and score 3). NAMPT, SIRT1, and DBC1 expression was detected in all dysplastic cells (Fig. 3b, c, d), with NAMPT being predominantly expressed in the nucleus (Fig. 3b).

Quantification of c-MYC expression in all classical adenomas (low and high-grade, Figs. 2a, 3a, 104 cases) revealed a staining score 1 in 21% (22/104), score 2 in

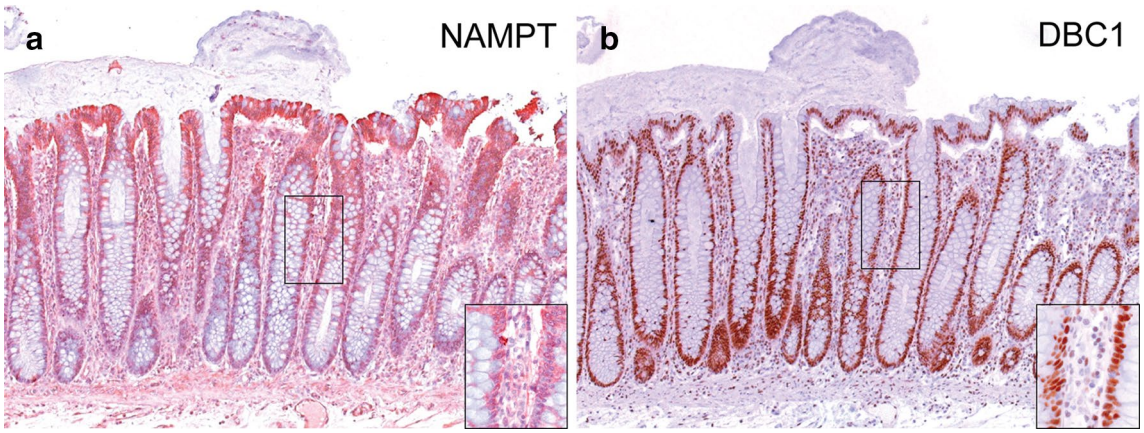

Fig. 1 NAMPT and DBC1 are expressed throughout the entire crypt in normal colorectal mucosa. Immunohistochemical staining of NAMPT (**a**) and DBC1 (**b**) in normal colorectal mucosa. Original magnification: ×100, inset ×600

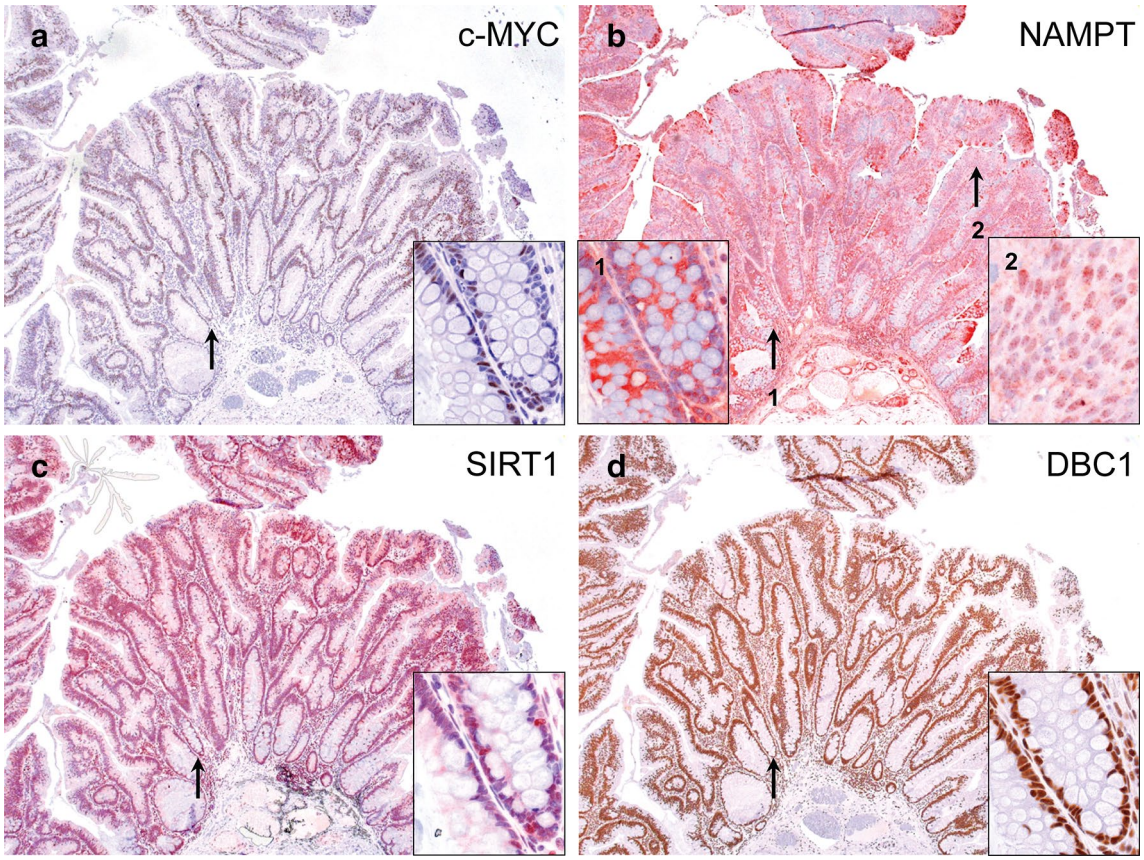

Fig. 2 c-MYC, NAMPT, SIRT1, and DBC1 are expressed in tubular adenomas with low-grade intraepithelial neoplasia. Immunohistochemical staining of c-MYC (**a**), NAMPT (**b**), SIRT1 (**c**), and DBC1 (**d**) in tubular adenomas with low-grade intraepithelial neoplasia. Original magnification: ×250, inset ×600

33% (34/104), and 46% (48/104) were classified score 3. Table 3 and Online Resource 4 provide the quantification of scoring c-MYC expression in all classical colorectal adenomas, including the *KRAS* mutation status. Within the group of tubular and tubulovillous adenomas, the expression of c-MYC was lower in lesions with low-grade intraepithelial neoplasia (tubular: 14% (4/28) of cases score 3, and tubulovillous: 26% (6/23) of cases score 3), than in lesions with high-grade intraepithelial neoplasia (tubular: 80% (8/10) cases score 3, tubulovillous 85% (17/20) score 3). In villous adenomas, a similar but less pronounced difference for c-MYC expression was observed (low-grade intraepithelial neoplasia: 50% (7/14) of cases score 3, high-grade intraepithelial neoplasia 67% (6/9) of cases score 3). Thus, c-MYC expression significantly correlated ($p = 0.00004$) with the grade of differentiation and malignant potential of the adenomas. However, we found no statistical correlation between c-MYC expression and *KRAS* mutational status ($p = 0.73$) (Online Resource 4, Table 3).

Expression of NAMPT and DBC1 in low and high-grade areas of serrated lesions

We have previously shown that c-MYC and SIRT1 are moderately to highly expressed in sessile-serrated colorectal adenomas with low-grade intraepithelial neoplasia, whereas most lesions with high-grade intraepithelial neoplasia exhibit high c-MYC and SIRT1 levels [7]. Since NAMPT is a positive regulator of SIRT1 activity, and DBC1 inhibits SIRT1 [23], we also assessed the expression of NAMPT and DBC1 in these sessile-serrated lesions. In sessile-serrated adenomas without intraepithelial neoplasia, NAMPT and DBC1 were expressed in all sections of the crypts, from the proliferative zone to the upper parts (Fig. 4a, b). In sessile-serrated adenomas with low-grade intraepithelial neoplasia (Fig. 4c, d), as well as in sessile-serrated adenomas with high-grade intraepithelial neoplasia (Fig. 4e, f), NAMPT and DBC1 were expressed in almost all dysplastic cells. Taken together, the correlated c-MYC, NAMPT, SIRT1, and DBC1 expression indicated that the positive feedback loop that was shown to connect the four proteins may be active in early colorectal adenomas, as well as in sessile-serrated lesions.

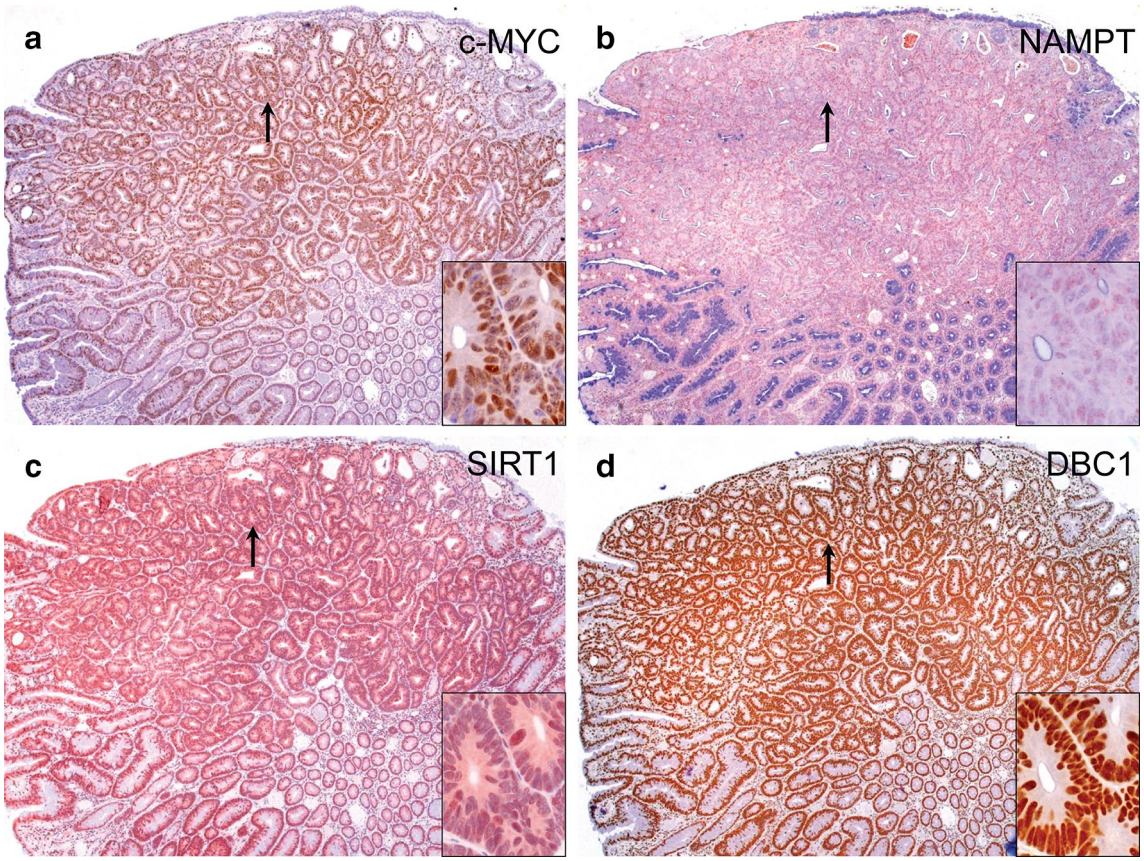

Fig. 3 c-MYC, NAMPT, SIRT1, and DBC1 are highly expressed in tubular adenomas with high-grade intraepithelial neoplasia. Immunohistochemical staining of c-MYC (**a**), NAMPT (**b**), SIRT1 (**c**), and DBC1 (**d**) in tubular adenomas with high-grade intraepithelial neoplasia. Original magnification: ×250, inset ×600

The upstream activation of c-MYC may be conferred by constitutive Wnt signaling, or oncogenic BRAF/K-Ras, respectively.

Genetic signatures associated with responses to NAMPT and SIRT1 inhibition using pharmacogenomic database analyses of CRC cell lines

Exploring the database of cancer cell lines CCLE, and the large pharmacological anti-cancer drug library GDSC, we addressed whether responsiveness of CRC cell lines to either NAMPT or SIRT1 inhibition is associated with molecular characteristics of single genes. We collected the mutational and copy number alteration (cna) profiles of forty-three CRC cell lines from CCLE and selected 26 commonly altered CRC genes [16]. We defined an altered gene status dependent on mutation and/or deletion/amplification and completed profiles for MSI and CIMP (Online Resource 3, for selection criteria of the 26 genes of interest and definition of gene status, see data acquisition section). Additionally, we extracted mRNA expression data of the 26 genes of interest, including *NAMPT*, and *SIRT1* from CCLE. Interestingly, copy number alterations were not consistently associated with changes in gene expression (Online Resource 5), suggesting additional mechanisms of transcriptional regulation.

We obtained IC-50 values of either NAMPT or SIRT1 inhibitors (FK866/ Daporinad, EX527/ Selisistat, respectively) from the GDSC project, resulting in 41/43 CCLE cell lines screened for FK866, and 39/43 for EX527 (Online Resource 3). *NAMPT* mRNA expression levels of the CRC cell lines and their FK866 IC-50 values did not correlate ($r = -0.008$) (Online Resource 6).

Upon stratification of the CRC cell lines in populations with or without a respective molecular alteration, we assessed whether these features impact on drug sensitivities. The total number of CRC cell lines per population and their responsiveness to FK866 is summarized in Online Resource 7. Alterations in the most commonly altered genes *APC, TP53, KRAS, FBXW7, SMAD4, ACVR2A, MSH6, RNF43, BRAF*, and MSI had no effect on the cell lines' vulnerability to NAMPT inhibition by FK866 (Fig. 5a–c and Online Resource 8a–g). However, mutation and/or deletion

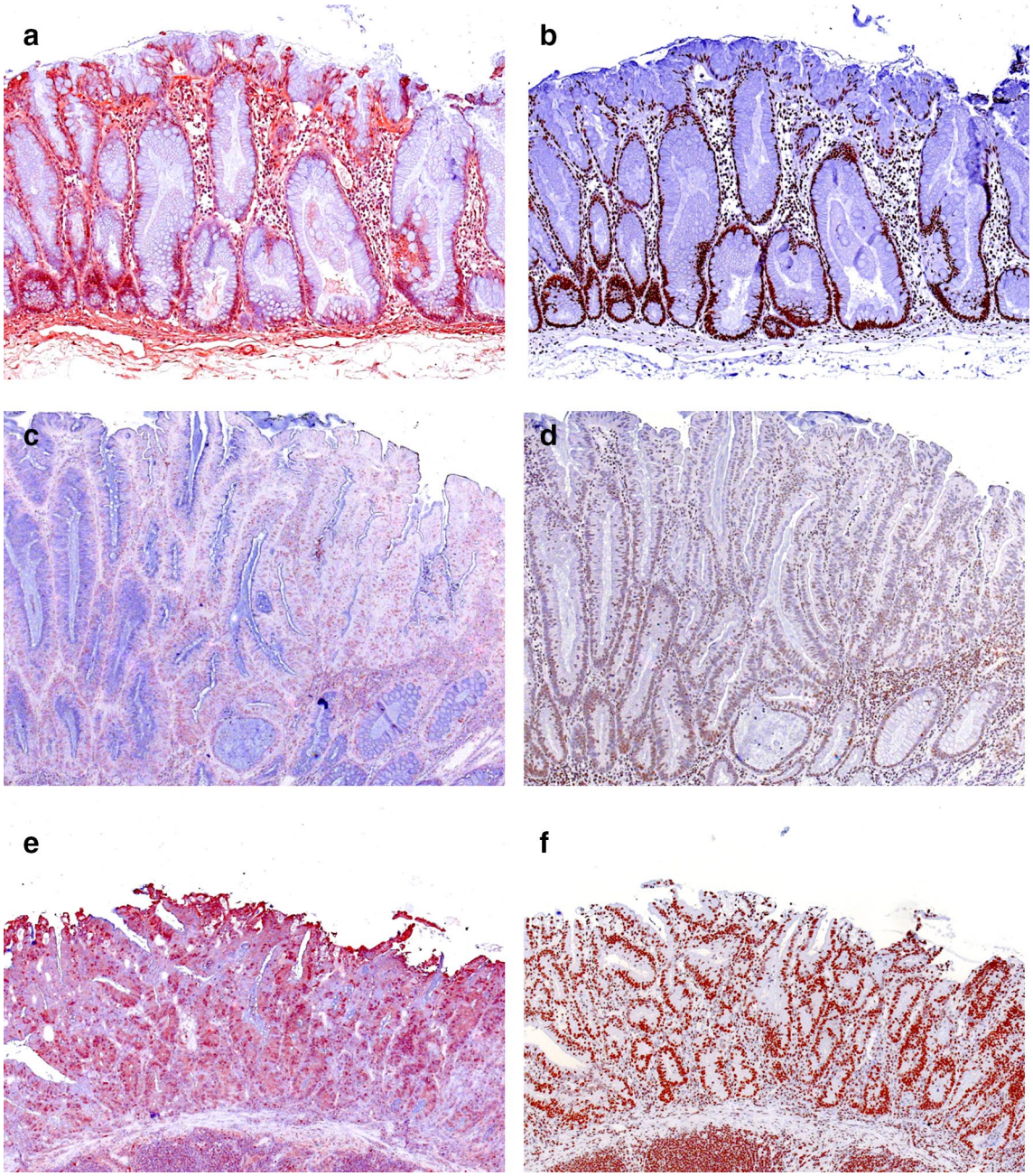

Fig. 4 NAMPT and DBC1 are expressed in sessile-serrated adenomas. Immunohistochemical staining of NAMPT and DBC1 in sessile-serrated adenomas without intraepithelial neoplasia (**a, b**), sessile-serrated adenomas with low-grade intraepithelial neoplasia (**c, d**), and sessile-serrated adenomas with high-grade intraepithelial neoplasia (**e, f**). Original magnification: ×100

in *TGFBR2* and *PTEN* were significantly associated with increased FK866 sensitivities (Fig. 5d, e).

Considering the wide range of FK866 IC-50 values (0.001 µM for HTC116 to 13.3 µM for HCC56), we subdivided the population in responsive cell lines (IC-50 FK866 < 0.01 µM, $n = 7$) and resistant cell lines (IC-50 FK866 > 1 µM, $n = 16$). The comparison of FK866 responsive versus resistant CRC cell lines revealed $RNF43^{mut/del}$ (low IC-50: 3/7 $RNF43^{mut/del}$, high IC-50: 3/16 $RNF43^{mut/del}$, $p = 0.318$), MSI (low IC-50: 3/7 MSI, high IC-50: 2/16 MSI, $p = 0.142$), and $BRAF^{mut/ampl}$ (low IC-50: 6/7 $BRAF^{mut/ampl}$, high IC-50: 6/17 $BRAF^{mut/ampl}$, $p = 0.069$) being preferentially present in responsive cell lines (Fig. 5f–h).

A tendency towards increased resistance to EX527 was observed for *KRAS* or *TP53* mutant cell lines (Fig. 6b, c), while alterations in *APC, FBXW7*, and *SMAD4* were significantly associated with increased resistance (Fig. 6a, d, e). Increased EX527 sensitivity was significantly associated

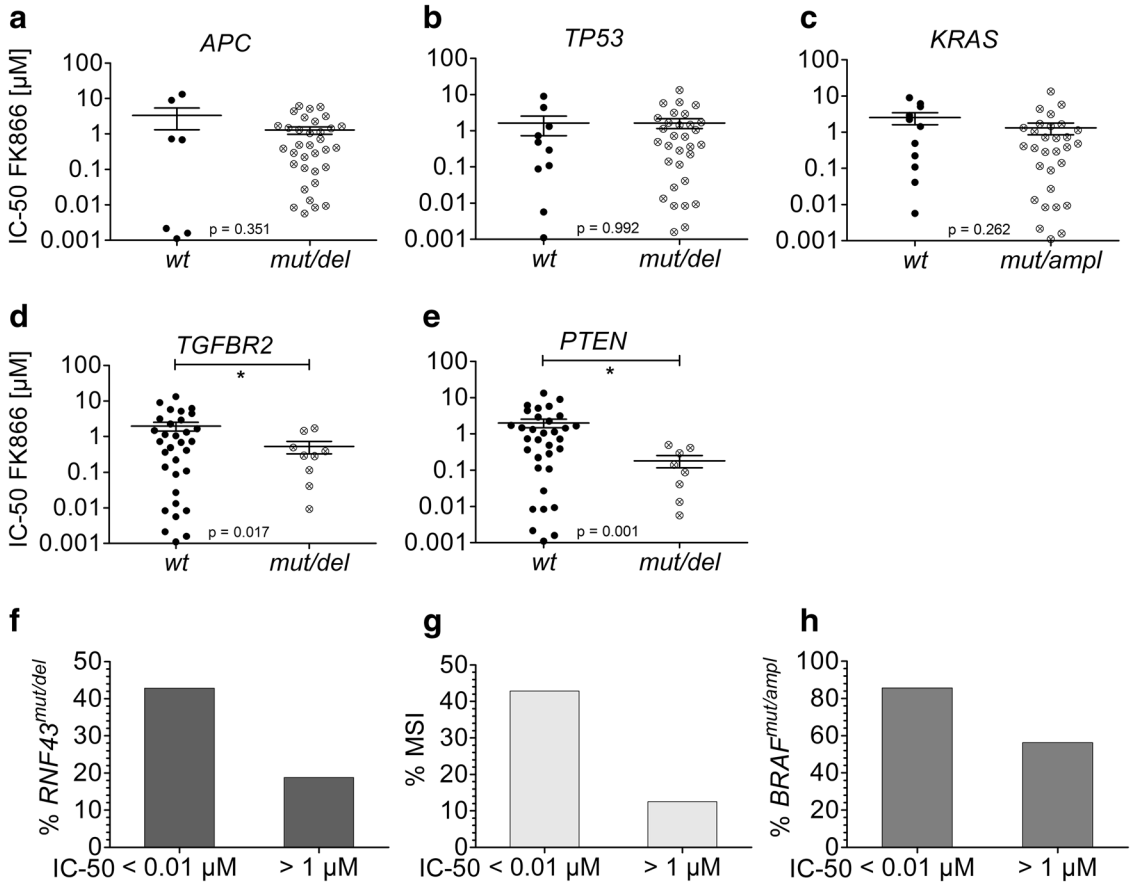

Fig. 5 FK866 sensitivity of CRC cell lines associates with $TGFBR2^{mut/del}$ and $PTEN^{mut/del}$. Comparative database analysis using FK866 IC-50 values from GDSC and mutation/ cna data from CCLE. Column scatter plot of FK866 IC-50 values plotted against presence or absence of $APC^{mut/del}$ (**a**), $TP53^{mut/del}$ (**b**), $KRAS^{mut/ampl}$ (**c**), $TGFBR2^{mut/del}$ (**d**), and $PTEN^{mut/del}$ (**e**). Mean+/− SEM. $*p < 0.05$ (unpaired *t* test). Stacked bar chart relating low (< 0.01 µM) and high (> 1 µM) FK866 IC-50 values to the proportion of cell lines altered in $RNF43^{mut/del}$ (**f**), MSI (**g**), and $BRAF^{mut/ampl}$ (**h**)

with $ACVR2A^{mut/del}$, $MSH6^{mut/del}$, $RNF43^{mut/del}$, and MSI (Fig. 6f–i), with $BRAF^{mut/ampl}$ displaying the same tendency (Fig. 6j). In contrast with FK866, $TGFBR2^{mut/del}$ and $PTEN^{mut/del}$ did not associate with increased EX527 responsiveness (Online Resource 9a, b). The total number of CRC cell lines harboring a respective alteration and their responsiveness to EX527 is given in Online Resource 10.

MSI CRCs have previously been associated with increased SIRT1 expression [5]. Since our data indicated that MSI is linked to an increased sensitivity towards SIRT1 inhibition, we sorted the 43 CRC cell lines for decreasing *SIRT1* mRNA expression levels and assigned cell lines with MSI or $RNF43^{mut/del}$ (Online Resource 11a). MSI and $RNF43^{mut/del}$ cell lines with their EX527 IC-50 value are depicted in Online Resource 12. We calculated the mean *SIRT1* expression over all cell lines (mean$n = 8.33$ RPKM (reads per kilobase per million mapped reads)) and determined a low *SIRT1* expressing population (*SIRT1* RPKM < mean, $n = 25$) and a high *SIRT1* expressing cell population (*SIRT1* RPKM > mean, $n = 18$). High SIRT1 expressing cell lines were more sensitive towards EX527 ($p = 0.16$, Online Resource 11b). Comparing high versus low *SIRT1* expressing cell lines revealed a significant association of $RNF43^{mut/del}$ (low *SIRT1*: 2/24 $RNF43^{mut/del}$, high *SIRT1*: 10/18 $RNF43^{mut/del}$, $p = 0.001$, Fig. 6k) and MSI (low *SIRT1*: 3/24 MSI, high *SIRT1*: 10/18 MSI, $p = 0.006$, Fig. 7l) to the high *SIRT1* expressing cell lines, with the same tendency for $BRAF^{mut/ampl}$ (low *SIRT1*: 8/24 $BRAF^{mut/ampl}$, high *SIRT1*: 8/18 $BRAF^{mut/ampl}$, $p = 0.531$, Fig. 6m). Mostly SIRT1 is regulated at the protein level [24], whereas here we identified a link between SIRT1 mRNA expression and MSI. Interestingly, mutations in *BRAF, MSH6, RNF43*, and MSI are characteristics for serrated route CRCs [17]. We observed an increased sensitivity of cell lines harboring these three alterations towards both, FK866 and EX527, suggesting that targeting NAMPT or SIRT1 may represent novel therapeutic opportunities especially for serrated CRCs.

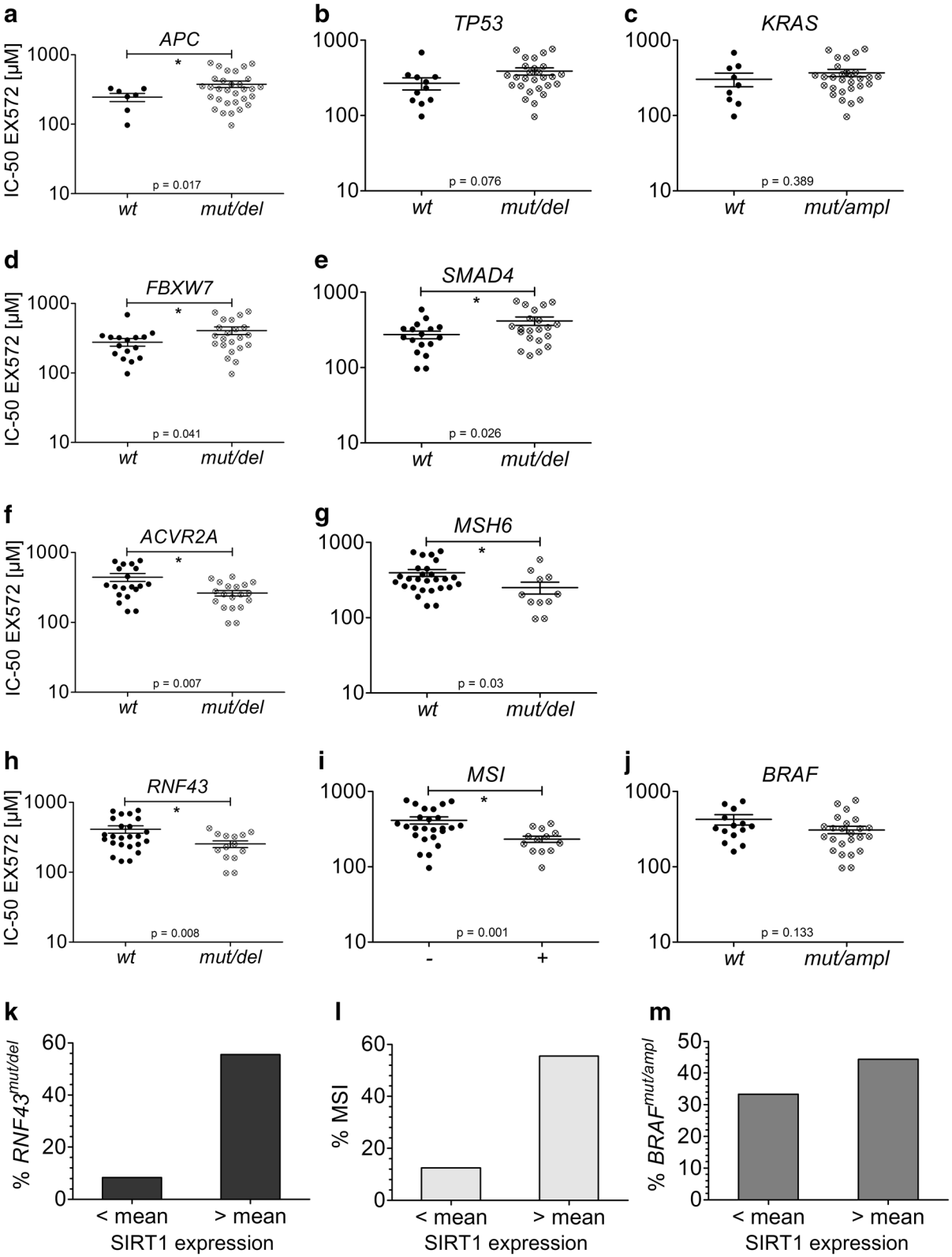
a
APC
IC-50 EX572 [µM]
1000
100
10
*
p = 0.017
wt
mut/del
b
TP53
p = 0.076
wt
mut/del
c
KRAS
p = 0.389
wt
mut/ampl
d
FBXW7
p = 0.041
wt
mut/del
e
SMAD4
p = 0.026
wt
mut/del
f
ACVR2A
p = 0.007
wt
mut/del
g
MSH6
p = 0.03
wt
mut/del
h
RNF43
p = 0.008
wt
mut/del
i
MSI
p = 0.001
-
+
j
BRAF
p = 0.133
wt
mut/ampl
k
% RNF43mut/del
60
40
20
0
< mean
> mean
SIRT1 expression
l
% MSI
60
40
20
0
< mean
> mean
SIRT1 expression
m
% BRAFmut/ampl
50
40
30
20
10
0
< mean
> mean
SIRT1 expression

◂**Fig. 6** EX527 sensitivity of CRC cell lines associates with *RNF43*$^{mut/del}$, MSI, and high *SIRT1* mRNA expression. Comparative database analysis using EX527 IC-50 values from GDSC and mutation/ cna/ RNA expression data from CCLE. Column scatter plot of EX527 IC-50 values plotted against presence or absence of *APC*$^{mut/del}$ (**a**), *TP53*$^{mut/del}$ (**b**), *KRAS*$^{mut/ampl}$ (**c**), *FBXW7*$^{mut/del}$ (**d**), *SMAD4*$^{mut/del}$ (**e**), *ACVR2A*$^{mut/del}$ (**f**), *MSH6*$^{mut/del}$ (**g**), *RNF43*$^{mut/del}$ (**h**), MSI (**i**), and *BRAF*$^{mut/ampl}$ (**j**). Mean+/− SEM. *$p < 0.05$ (unpaired *t* test). Stacked bar chart relating low *SIRT1* expressing (RPKM < mean, $n = 25$) or high *SIRT1* expressing (RPKM > mean, $n = 18$) cell lines to alterations in *RNF43*$^{mut/del}$ (**k**), MSI (**l**), *BRAF*$^{mut/ampl}$ (**m**). Mean *SIRT1* RPKM was calculated over all cell lines (mean$n = 8.33$ RPKM, see also Online Resource 11). *$p < 0.05$ (Fisher's exact test)

Discussion

In the normal mucosa of the colon, c-MYC is limited to the proliferative zone in the basal third of the crypts where it is essential for intestinal crypt formation [7]. The β-catenin/TCF-4/LEF1 complex transcriptionally induces *c-MYC* in conventional colorectal adenomas [25] leading to ubiquitous expression of c-MYC we observed in all different adenoma subgroups. Compared to normal colon mucosa, low-grade and high-grade intraepithelial neoplasia display increasingly elevated c-MYC levels, reflecting the role of c-MYC in tumor initiation as demonstrated in various mouse models (reviewed in [26]). Additionally, increased c-MYC expression and a high mutation rate of *KRAS* in tubulovillous, and even higher in villous adenomas compared to tubular adenomas suggested that high c-MYC expression and mutant *KRAS* correlate with aggressiveness. Accordingly, c-MYC is higher expressed in moderately and poorly differentiated carcinomas compared to well-differentiated tumors, which is in agreement with the role of c-MYC in tumor progression [26].

These data are in accordance with previous studies that discussed mutant *KRAS* to contribute to an extension and elongation of crypt morphology leading to villous architecture by enhancing proliferation and/or providing a survival advantage [27]. *KRAS* mutation has been suggested to induce stem cell-like programs contributing to human intestinal cancer initiation [28] and to determine the impact of Wnt activity on stemness phenotypes. Furthermore, *KRAS* mutation has also been linked to decreased proliferation and senescence [29], putatively explaining why we did not detect a statistically significant correlation of the *KRAS* mutational status and c-MYC expression in our collection.

In a previous study, we revealed that in the alternative, serrated route to CRC, high c-MYC levels were associated with mutant K-Ras or B-Raf, or in a minor fraction, with Wnt pathway activation [7]. Increasing high c-MYC expression levels characterized serrated lesions irrespective of the histologic subtype, or of the side of localization [7]. Our data presented here suggest that enabling c-MYC activation, either transcriptionally by deregulation of Wnt signaling, or post-transcriptionally through oncogenic K-Ras or B-Raf, is an early event in both the classical route, as well as in the serrated route to CRC. As a result, all CRC subtypes, irrespective of the initial molecular alteration, are characterized by a c-MYC-target gene signature [16].

Integrating our previous finding of elevated SIRT1 expression in conventional CRCs [4], we now document, that already early tumor lesions are characterized by high SIRT1 expression. High expression of SIRT1 in CRCs has been linked to an MSI and CpG methylation phenotype, associated with bad prognosis, expression of the stem cell marker CD133, EMT, and metastasis [5, 30, 31]. In early adenomas, deregulation of c-MYC may lead to TP53 activation [32]. However, the concomitant induction of SIRT1 may prevent a full blown TP53 response, thus antagonizing apoptosis and senescence, and allowing for permanent proliferation [4]. Therefore, collaboration of elevated c-MYC and SIRT1 in conventional and serrated lesions may promote cell survival and tumor progression by supporting c-MYC function and blocking pro-apoptotic pathways through the SIRT1 feedback [4].

As we have shown previously, c-MYC induces SIRT1 which is accompanied by the activation of *NAMPT*, an elevated production of the SIRT1 cofactor NAD^+ by NAMPT, and by sequestration of the endogenous SIRT1 inhibitor protein DBC1/CCAR2 [4]. Here, we demonstrated that NAMPT is expressed in all conventional adenomas and serrated lesions with a more accentuated expression in the cytoplasm in basal areas and a more nuclear localization in apical parts, and high-grade areas. Expression of NAMPT is more abundant in the cytoplasm in proliferating cells, than in arrested or differentiated cells, where it is predominantly localized in the nucleus [33]. This points to a cell cycle-dependent subcellular localization of NAMPT in non-transformed cells. In high-grade areas of CRC tissue, however, nuclear NAMPT may reflect increased local NAD^+ needs presumably due to a higher activity of NAD^+ consuming nuclear SIRT1 and PARP1 enzymes (reviewed in [34]).

Despite the differential sub-cellular localization, we found no evidence for an upregulation of NAMPT in colorectal adenomas above the already high expression in the normal mucosa. It was expressed along the whole crypt in the normal colon. High NAMPT expression at the top of the crypts in the intestine may be the consequence of hypoxic conditions, along with the HIF1α activation in this area [35], and the transcriptional induction of NAMPT by HIF1α [36]. It is therefore conceivable, that high NAMPT expression in intestinal villi reflects specific metabolic needs of cells in these hypoxic areas. Together, these observations support a function of NAMPT normal intestinal epithelial cell homeostasis in humans, which is in agreement with a previous report analyzing *nampt* deficiency in mice [37].

As we have shown before, upon c-MYC deregulation, the DBC1/c-MYC protein interaction leads to sequestration of DBC1 from binding to SIRT1 [4]. In agreement with this, binding of DBC1 to SIRT1 is weak or absent in tumor cells [38]. We asked, whether reduced DBC1/CCAR2 expression may also support pro-tumorigenic SIRT1 functions. However, according to our results regulation of DBC1 expression does not contribute to SIRT1 activation in adenomas.

FK866, an inhibitor of NAMPT, leads to ATP depletion and cell death in a broad spectrum of cancer cell lines. Initial clinical trials revealed dose-limiting side effects, urging for chemical improvement of NAMPT inhibitors (reviewed in [10]) and stratification of patients according to predictive markers. In contrast, despite intensive *in vitro* and pre-clinical analyses, and the demonstration that SIRT1 inhibition may represent a therapeutic strategy for eliminating cancer stem cells and overcome drug-resistance [39, 40], SIRT1 inhibitors have not been tested in clinical trials for cancer therapy so far.

Since CRC cell lines have recently been shown to mirror the genomic profile of primary CRCs [12, 20], they are valuable resources for pre-clinical drug studies. Systematic screening of large pharmacological anti-cancer drug libraries (GDSC) allowed the integration of heterogeneous molecular data collected by CCLE with drug responses. The machine learning approach developed by Iorio *et al*. most reliably predicted drug responses based on (tissue specific) gene expression [12]. However, genomic profiling of clinical cancer patients so far relies on mutations and copy number alterations of mostly cancer-related genes. In our study, we integrated the mutational profile of cancer-related genes and their copy number information using CRC cell lines as pre-clinical models.

Thereby, we identified inactivating mutations and deletions in *TGFBR2* and *PTEN* being significantly associated with FK866 sensitivity. Correspondingly, activating mutations in *PIK3CA* were also linked to lower IC-50 values, albeit not to a significant degree. *TGFBR2* mutations are frequently detected and linked to MSI in colon cancer, indicating that sensitivity may be higher in cell lines derived from the serrated route CRC [41]. Mutations in *TGFBR2* abrogate anti-proliferative TGFβ signaling and prevent SMAD4 to transcriptionally repress c-MYC [42]. Likewise, loss of *PTEN* results in increased c-MYC abundance through aberrant signaling of the growth and survival kinase PI3K [43]. Thus, alterations in *TGFBR2, PTEN*, and *PIK3CA* collectively contribute to elevated c-MYC levels, and putatively to increased NAMPT and SIRT1 activity [4] rendering them more vulnerable to inhibition, as our data have revealed for SIRT1. FK866 sensitizing mutations in *PTEN* or *TGFBR2* were both detected in approximately ~ 20% of CRC cancer cell lines. In a collection of 981 primary and metastatic colorectal adenocarcinomas, their mutation frequency is lower (8% (*PTEN*), 4% (*TGFBR2*)) (MSK-IMPACT Clinical Sequencing Cohort) [44], suggesting that approximately 12% of CRC patients may qualify for therapeutic interfering with NAMPT function.

High concentrations of EX527 also inhibit SIRT2 and SIRT3. It has been shown that SIRT1 inhibition alone does only have minor effects on cell growth, while the combined inhibition of SIRT1 and SIRT2 performs better [45]. Indeed, IC-50 values of the assessed CRC cell lines were generally > 100 µM, implying that the EX527 effects probably result from combined inhibition of SIRT1 and other sirtuins. We found that sensitivity towards SIRT inhibition was conferred by molecular alterations in *ACVR2A, MSH6, RNF43*, and MSI. These alterations were also preferentially found in the highly sensitive population during NAMPT inhibition. Again, somatic alterations in *RNF43, MSH6*, and MSI specify the serrated route CRC subtype. In agreement with this, a significant resistance to EX527 was associated with mutant *APC*, characterizing the majority of classical route CRC. The reason for increased sensitivity of serrated route CRC cells however remains unclear since no direct link between components of the feedback loop and any of the identified markers is known. Similarly, it was unexpected that cell lines representing potential descendants from serrated route tumors with high MSI, which typically have bad response rates to therapies and a better prognosis than MSS tumors were specifically sensitive towards NAMPT and SIRT1 inhibitors. However, single predictor associations often produce unexplainable relations of gene alterations and drug responsiveness, as the interaction between biological pathways and components is neglected. Consequently, there is a need for more accurate models that take this interplay into account.

Taken together, we provide evidence that the c-MYC–NAMPT–SIRT1 positive feedback loop is involved in the development of the two main pathways to colorectal carcinoma, the conventional adenoma–carcinoma sequence, and the alternative, serrated pathway. Its presence in early-stage human colon adenomas points to a potential involvement in driving neoplasia. Thereby, oncogenic functions of c-MYC and properties of SIRT1, such as antagonizing apoptosis and senescence, supporting c-MYC function and/or epigenetic regulation may contribute to tumorigenesis. According to our database analyses of pharmacogenomics, the components of the feedback loop are necessary for the maintenance of CRC and may represent novel targets for future therapies, being admitted as monotherapy or as combination therapy. Most importantly, the molecular markers associated with therapy responsiveness and resistance may aid patient stratification for future clinical trials.

Acknowledgements This study was supported by the German Research Foundation (Deutsche Forschungsgemeinschaft) Grant (# Me1719/3-1)

(support to AM). We thank A. Heier for her expert support and experimental assistance.

Compliance with ethical standards

Conflict of interest The authors declare that they have no conflict of interest.

Research involving human participants Data and specimens were anonymized, and the need for consent was waived by the institutional ethics committee of the Medical Faculty of the Ludwig-Maximilians University.

References

1. Vogelstein B, Fearon ER, Hamilton SR, Kern SE, Preisinger AC, Leppert M, et al. Genetic alterations during colorectal-tumor development. N Engl J Med. 1988;319(9):525–32. https://doi.org/10.1056/NEJM198809013190901.
2. Dang CV. MYC on the path to cancer. Cell. 2012;149(1):22–35. https://doi.org/10.1016/j.cell.2012.03.003.
3. Menssen A, Hermeking H. c-MYC and SIRT1 locked in a vicious cycle. Oncotarget. 2012;3(2):112–3. https://doi.org/10.18632/oncotarget.440.
4. Menssen A, Hydbring P, Kapelle K, Vervoorts J, Diebold J, Luscher B, et al. The c-MYC oncoprotein, the NAMPT enzyme, the SIRT1-inhibitor DBC1, and the SIRT1 deacetylase form a positive feedback loop. Proc Natl Acad Sci USA. 2012;109(4):E187-96. https://doi.org/10.1073/pnas.1105304109.
5. Nosho K, Shima K, Irahara N, Kure S, Firestein R, Baba Y, et al. SIRT1 histone deacetylase expression is associated with microsatellite instability and CpG island methylator phenotype in colorectal cancer. Mod Pathol. 2009;22(7):922–32. https://doi.org/10.1038/modpathol.2009.49.
6. Leko V, Park GJ, Lao U, Simon JA, Bedalov A. Enterocyte-specific inactivation of SIRT1 reduces tumor load in the APC(+/min) mouse model. PLoS ONE. 2013;8(6):e66283. https://doi.org/10.1371/journal.pone.0066283.
7. Kriegl L, Vieth M, Kirchner T, Menssen A. Up-regulation of c-MYC and SIRT1 expression correlates with malignant transformation in the serrated route to colorectal cancer. Oncotarget. 2012;3(10):1182–93. https://doi.org/10.18632/oncotarget.628.
8. Noffsinger AE. Serrated polyps and colorectal cancer: new pathway to malignancy. Annu Rev Pathol. 2009;4:343–64. https://doi.org/10.1146/annurev.pathol.4.110807.092317.
9. Chalkiadaki A, Guarente L. The multifaceted functions of sirtuins in cancer. Nat Rev Cancer. 2015;15(10):608–24. https://doi.org/10.1038/nrc3985.
10. Sampath D, Zabka TS, Misner DL, O'Brien T, Dragovich PS. Inhibition of nicotinamide phosphoribosyltransferase (NAMPT) as a therapeutic strategy in cancer. Pharmacol Ther. 2015;151:16–31. https://doi.org/10.1016/j.pharmthera.2015.02.004.
11. Barretina J, Caponigro G, Stransky N, Venkatesan K, Margolin AA, Kim S, et al. The Cancer Cell Line Encyclopedia enables predictive modelling of anticancer drug sensitivity. Nature. 2012;483(7391):603–7. https://doi.org/10.1038/nature11003.
12. Iorio F, Knijnenburg TA, Vis DJ, Bignell GR, Menden MP, Schubert M, et al. A landscape of pharmacogenomic interactions in cancer. Cell. 2016;166(3):740–54. https://doi.org/10.1016/j.cell.2016.06.017.
13. Yang W, Soares J, Greninger P, Edelman EJ, Lightfoot H, Forbes S, et al. Genomics of Drug Sensitivity in Cancer (GDSC): a resource for therapeutic biomarker discovery in cancer cells. Nucleic Acids Res. 2013;41(Database issue):D955-61. https://doi.org/10.1093/nar/gks1111.
14. Hamilton SRBF, Boffetta P, Ilyas M, Nakamura SI, Quirke P, Riboli E, Sobin LH. Carcinoma of the colon and rectum. In: Bosman FT CF, Hruban RH, Theise ND, editor. WHO Classification of Tumors of the Digestive System. Lyon (France): International Agency for Research on cancer (IARC); 2010. p. 139.
15. Torlakovic EE, Gomez JD, Driman DK, Parfitt JR, Wang C, Benerjee T, et al. Sessile serrated adenoma (SSA) vs. traditional serrated adenoma (TSA). Am J Surg Pathol. 2008;32(1):21–9. https://doi.org/10.1097/PAS.0b013e318157f002.
16. Cancer Genome Atlas N. Comprehensive molecular characterization of human colon and rectal cancer. Nature. 2012;487(7407):330–7. https://doi.org/10.1038/nature11252.
17. Bond CE, McKeone DM, Kalimutho M, Bettington ML, Pearson SA, Dumenil TD, et al. RNF43 and ZNRF3 are commonly altered in serrated pathway colorectal tumorigenesis. Oncotarget. 2016;7(43):70589–600. https://doi.org/10.18632/oncotarget.12130.
18. Slattery ML, Herrick JS, Mullany LE, Samowitz WS, Sevens JR, Sakoda L, et al. The co-regulatory networks of tumor suppressor genes, oncogenes, and miRNAs in colorectal cancer. Genes Chromosomes Cancer. 2017;56(11):769–87. https://doi.org/10.1002/gcc.22481.
19. Ueda M, Iguchi T, Masuda T, Komatsu H, Nambara S, Sakimura S, et al. Up-regulation of SLC9A9 promotes cancer progression and is involved in poor prognosis in colorectal cancer. Anticancer Res. 2017;37(5):2255–63. https://doi.org/10.21873/anticanres.11562.
20. Berg KCG, Eide PW, Eilertsen IA, Johannessen B, Bruun J, Danielsen SA, et al. Multi-omics of 34 colorectal cancer cell lines - a resource for biomedical studies. Mol Cancer. 2017;16(1):116. https://doi.org/10.1186/s12943-017-0691-y.
21. Mouradov D, Sloggett C, Jorissen RN, Love CG, Li S, Burgess AW, et al. Colorectal cancer cell lines are representative models of the main molecular subtypes of primary cancer. Cancer Res. 2014;74(12):3238–47. https://doi.org/10.1158/0008-5472.CAN-14-0013.
22. Yadamsuren EA, Nagy S, Pajor L, Lacza A, Bogner B. Characteristics of advanced- and non advanced sporadic polypoid colorectal adenomas: correlation to KRAS mutations. Pathol Oncol Res. 2012;18(4):1077–84. https://doi.org/10.1007/s12253-012-9547-3.
23. Kim JE, Chen J, Lou Z. DBC1 is a negative regulator of SIRT1. Nature. 2008;451(7178):583–6. https://doi.org/10.1038/nature06500.
24. Milner J. Cellular regulation of SIRT1. Curr Pharm Des. 2009;15(1):39–44.
25. He TC, Sparks AB, Rago C, Hermeking H, Zawel L, da Costa LT, et al. Identification of c-MYC as a target of the APC pathway. Science. 1998;281(5382):1509–12.
26. Gabay M, Li Y, Felsher DW. MYC activation is a hallmark of cancer initiation and maintenance. Cold Spring Harbor Perspect Med. 2014;4(6). https://doi.org/10.1101/cshperspect.a014241.
27. Feng Y, Bommer GT, Zhao J, Green M, Sands E, Zhai Y, et al. Mutant KRAS promotes hyperplasia and alters differentiation in the colon epithelium but does not expand the presumptive stem cell pool. Gastroenterology. 2011;141(3):1003–13 e1–10. https://doi.org/10.1053/j.gastro.2011.05.007.
28. Le Rolle AF, Chiu TK, Zeng Z, Shia J, Weiser MR, Paty PB, et al. Oncogenic KRAS activates an embryonic stem cell-like program in human colon cancer initiation. Oncotarget. 2016;7(3):2159–74. https://doi.org/10.18632/oncotarget.6818.
29. Giaretti W, Rapallo A, Geido E, Sciutto A, Merlo F, Risio M, et al. Specific K-ras2 mutations in human sporadic colorectal adenomas are associated with DNA near-diploid aneuploidy and inhibition

of proliferation. Am J Pathol. 1998;153(4):1201–9. https://doi.org/10.1016/S0002-9440(10)65664-7.
30. Chen X, Sun K, Jiao S, Cai N, Zhao X, Zou H, et al. High levels of SIRT1 expression enhance tumorigenesis and associate with a poor prognosis of colorectal carcinoma patients. Sci Rep. 2014;4:7481. https://doi.org/10.1038/srep07481.
31. Cheng F, Su L, Yao C, Liu L, Shen J, Liu C, et al. SIRT1 promotes epithelial-mesenchymal transition and metastasis in colorectal cancer by regulating Fra-1 expression. Cancer Lett. 2016;375(2):274–83. https://doi.org/10.1016/j.canlet.2016.03.010.
32. Finch AJ, Soucek L, Junttila MR, Swigart LB, Evan GI. Acute overexpression of Myc in intestinal epithelium recapitulates some but not all the changes elicited by Wnt/beta-catenin pathway activation. Mol Cell Biol. 2009;29(19):5306–15. https://doi.org/10.1128/MCB.01745-08.
33. Kitani T, Okuno S, Fujisawa H. Growth phase-dependent changes in the subcellular localization of pre-B-cell colony-enhancing factor. FEBS Lett. 2003;544(1–3):74–8.
34. Imai S, Guarente L. NAD+ and sirtuins in aging and disease. Trends Cell Biol. 2014;24(8):464–71. https://doi.org/10.1016/j.tcb.2014.04.002.
35. Taylor CT, Colgan SP. Hypoxia and gastrointestinal disease. J Mol Med (Berl). 2007;85(12):1295–300. https://doi.org/10.1007/s00109-007-0277-z.
36. Bae SK, Kim SR, Kim JG, Kim JY, Koo TH, Jang HO, et al. Hypoxic induction of human visfatin gene is directly mediated by hypoxia-inducible factor-1. FEBS Lett. 2006;580(17):4105–13. https://doi.org/10.1016/j.febslet.2006.06.052.
37. Zhang LQ, Van Haandel L, Xiong M, Huang P, Heruth DP, Bi C, et al. Metabolic and molecular insights into an essential role of nicotinamide phosphoribosyltransferase. Cell Death Dis. 2017;8:e2705. https://doi.org/10.1038/cddis.2017.132.
38. Kim JE, Lou Z, Chen J. Interactions between DBC1 and SIRT 1 are deregulated in breast cancer cells. Cell Cycle. 2009;8(22):3784–5. https://doi.org/10.4161/cc.8.22.10055.
39. Li L, Wang L, Li L, Wang Z, Ho Y, McDonald T, et al. Activation of p53 by SIRT1 inhibition enhances elimination of CML leukemia stem cells in combination with imatinib. Cancer Cell. 2012;21(2):266–81. https://doi.org/10.1016/j.ccr.2011.12.020.
40. Wang Z, Yuan H, Roth M, Stark JM, Bhatia R, Chen WY. SIRT1 deacetylase promotes acquisition of genetic mutations for drug resistance in CML cells. Oncogene. 2013;32(5):589–98. https://doi.org/10.1038/onc.2012.83.
41. Markowitz S, Wang J, Myeroff L, Parsons R, Sun L, Lutterbaugh J, et al. Inactivation of the type II TGF-beta receptor in colon cancer cells with microsatellite instability. Science. 1995;268(5215):1336–8.
42. Massague J. TGF-beta signal transduction. Annu Rev Biochem. 1998;67:753–91. https://doi.org/10.1146/annurev.biochem.67.1.753.
43. Hann SR. Role of post-translational modifications in regulating c-Myc proteolysis, transcriptional activity and biological function. Semin Cancer Biol. 2006;16(4):288–302. https://doi.org/10.1016/j.semcancer.2006.08.004.
44. Zehir A, Benayed R, Shah RH, Syed A, Middha S, Kim HR, et al. Mutational landscape of metastatic cancer revealed from prospective clinical sequencing of 10,000 patients. Nat Med. 2017;23(6):703–13. https://doi.org/10.1038/nm.4333.
45. Peck B, Chen CY, Ho KK, Di Fruscia P, Myatt SS, Coombes RC, et al. SIRT inhibitors induce cell death and p53 acetylation through targeting both SIRT1 and SIRT2. Mol Cancer Ther. 2010;9(4):844–55. https://doi.org/10.1158/1535-7163.MCT-09-0971.